

Review

A Review on the Fabrication of Hierarchical ZnO Nanostructures for Photocatalysis Application

Yi Xia ^{1,2,3}, Jing Wang ^{2,*}, Ruosong Chen ², Dali Zhou ^{1,*} and Lan Xiang ^{2,*}

¹ College of Material Science and Engineering, Sichuan University, Chengdu 610065, China; xiayi0125@stu.scu.edu.cn

² Department of Chemical Engineering, Tsinghua University, Beijing 100084, China; chenruosongxz@163.com

³ Research Center for Analysis and Measurement, Kunming University of Science and Technology, Kunming 650093, China

* Correspondence: wangjingflotu@gmail.com (J.W.); zdl@scu.edu.cn (D.Z.); xianglan@mail.tsinghua.edu.cn (L.X.); Tel.: +86-10-6278-8984 (J.W., D.Z. & L.X.); Fax: +86-10-6277-2051 (J.W., D.Z. & L.X.)

Academic Editor: Monica Distaso

Received: 20 October 2016; Accepted: 8 November 2016; Published: 16 November 2016

Abstract: Semiconductor photocatalysis provides potential solutions for many energy and environmental-related issues. Recently, various semiconductors with hierarchical nanostructures have been fabricated to achieve efficient photocatalysts owing to their multiple advantages, such as high surface area, porous structures, as well as enhanced light harvesting. ZnO has been widely investigated and considered as the most promising alternative photocatalyst to TiO₂. Herein, we present a review on the fabrication methods, growth mechanisms and photocatalytic applications of hierarchical ZnO nanostructures. Various synthetic strategies and growth mechanisms, including multistep sequential growth routes, template-based synthesis, template-free self-organization and precursor or self-templating strategies, are highlighted. In addition, the fabrication of multicomponent ZnO-based nanocomposites with hierarchical structures is also included. Finally, the application of hierarchical ZnO nanostructures and nanocomposites in typical photocatalytic reactions, such as pollutant degradation and H₂ evolution, is reviewed.

Keywords: hierarchical nanostructure; ZnO; fabrication; photocatalysis

1. Introduction

Various semiconductor nanomaterials have been widely used to solve energy and environment problems with their excellent photocatalytic properties [1–3]. In recent years, many researchers have focused on the fabrication of hierarchical semiconductor nanostructures and nanocomposites owing to their advantages, including high surface area, porous structures, as well as enhanced light harvesting, etc. [4]. Particularly, zinc oxide (ZnO) has attracted considerable attention as an efficient and promising candidate in photocatalytic applications because of its low cost, non-toxicity and high quantum yields [5–7].

Up to now, several reviews have been published on the fabrication strategy of hierarchical photocatalysts with various morphologies. However, only a small part mentioned the synthesis of hierarchical ZnO materials in photocatalytic application [4,8–10]. In addition, especially in the photocatalytic application of ZnO, most of the previous reviews are limited to low dimension (0D, 1D and 2D) ZnO nanostructures, where reviews about hierarchical ZnO nanostructures are still insufficient.

Herein, we present a review on the fabrication of hierarchical ZnO nanostructures for photocatalytic application. First, the advantages of ZnO hierarchical photocatalysts are discussed. Then, various synthetic strategies towards different hierarchical ZnO nanostructures and nanocomposites

are reviewed, including multistep sequential growth routes, template-based synthesis, template-free self-organization and precursor or self-templating strategies. The fabrication of nano-architected ZnO with hollow, porous and bio-inspired structures is also included. Moreover, the design and syntheses of ZnO-based hierarchical nanocomposites are highlighted. Finally, photocatalysis applications of hierarchical ZnO nanostructures and nanocomposites for photocatalytic processes, such as pollutant degradation and H₂ production, are briefly discussed.

2. Advantages of Hierarchical ZnO Nanostructures and Nanocomposites

2.1. High Surface Area and Porous Structures

The surface area and porous structures of semiconductor nanostructures play important roles in their photocatalytic activity [11–13]. Many researches have demonstrated that hierarchical nanostructures with a high surface area [14–16] showed better photocatalytic properties than those of conventional materials. Low dimensional ZnO nanostructures, such as nanoparticles, nanorods, nanosheets, nanotetrapods, etc. [17], were usually found to have a small surface area (typically <10 m²/g). In contrast, hierarchical nanostructures usually exhibited high surface to volume ratios, a large accessible surface area and better permeability, which could not only provide abundant active adsorption sites and photocatalytic reaction sites [18], but also improve the uniformity of the active sites distribution in the photocatalysts [4]. In some case, the increased surface area could also contribute to the increase of surface defects, which may act as active sites for photocatalytic reactions. We have recently developed a facile ultra-rapid solution method to fabricate ZnO nanosheets with a tunable BET surface area and rich oxygen-vacancy defects. The as-prepared ZnO nanosheets were rich in oxygen-vacancies, and the increased BET surface area led to a further increase of surface oxygen-vacancy concentration. The rich oxygen-vacancies promoted the visible-light absorption of the ZnO nanosheets, leading to high photocatalytic activities towards the degradation of rhodamine B, about 11-times higher than that of ZnO nanoparticles with few oxygen defects [19]. The design of hierarchical nanostructures constructed from nano-scaled building blocks possessing interconnected pores can also result in the increase surface areas. For instance, hierarchical ZnO porous structures with high specific surface areas >500 m²/g could be produced using MOF as the precursor [20]. It was also demonstrated that the formation of porous networks in hierarchical structures would result in the creation of more efficient channels for the transport of reactant molecules, which facilitate the diffusion process [21–24].

2.2. Enhanced Light Harvesting

Increasing the light-harvesting ability of photocatalysts can greatly enhance the photocatalytic property [11]. The hierarchically-structured photocatalysts with interconnected pores could increase the number of light traveling paths and thereby result in increased interaction time and enhanced absorption efficiency, especially for core-shell and hollow structures. For example, hierarchical ZnO hollow spheroids exhibited enhanced photocatalytic dye degradation activity due to more efficient utilization of light through the multiple light reflections in the hollow structures [25]. Carbon-doped porous ZnO nanoarchitectures [26] showed enhanced photocatalytic H₂-evolution activities owing to the increased light path length within the pore-channel networks. The enhanced light absorption was attributed to the so-called light-scattering effects [27], which were also widely employed in dye-sensitized solar cells [28]. Generally, the interconnected accessible pore channels in the hierarchical structures were crucial for promoting the light-harvesting efficiency. Therefore, the construction of hierarchical porous nanostructures was particularly effective to increase the light harvesting.

2.3. Synergistic Nano-Building Blocks and Multi-Components

The superior photocatalytic performance of the hierarchical micro/nanostructures could be also related to their self-supporting structural features, which could overcome the agglomeration and sintering problems observed in the case of conventional nanosized ZnO [28,29]. Moreover,

enhanced efficiency for charge transfer and separation could be expected among these well-organized nanoscale building blocks, especially when heterostructured nanocomposites were further constructed. These above advantages of hierarchical ZnO nanostructures have recently motivated researchers engaged in developing various synthesis routes of hierarchical ZnO nanostructures, which will be summarized in the following section.

3. Synthetic Strategies of Hierarchical ZnO Nanostructures and Nanocomposites

3.1. Multistep Sequential Growth Routes

A multistep strategy can be used to fabricate many desired hierarchical structures, such as branched nanostructures, nanosheet-nanorod structures, core-shell structures, etc., from either multi-independent processes or from a one-pot solution with continuous processes [9]. Based on the preparation processes, multi-step self-assembly can be classified into two or more typical types, namely multi-step self-assembly with multi-discontinuous processes and multi-step self-assembly completed in one-pot solution syntheses. Compared to the conventional one-step assembly, the multi-step sequential growth routes allow the combination of multiple nanoscale building blocks. Moreover, this approach could also be employed in the formation of heterostructures or hybrid nanomaterials in a cost-effective way [8].

Multi-step self-assembly with multi-discontinuous processes involves the preparation of primary low dimensional structures, followed by the formation of hierarchical structures via sequential modification of primary structures. For instance, Zhang et al. [30] reported a multi-sequential nucleation and growth route for the systematic building of a complex ZnO hierarchical nanostructure by combining 1D units under a solution method. The growth processes included three steps: preparation of primary ZnO rods, oriented growth of nanoplates on the columnar facets of primary ZnO rods through a low temperature solution method and the formation of the final complex ZnO hierarchical structures via further hydrothermal treatment. The schematic illustration and pictorial presentation of samples are shown in Figure 1. Using a similar nucleation and growth protocol, brush-like hierarchical ZnO nanostructures assembled from initial 1D ZnO nanostructures were prepared by Zhang et al. [31] via a simple hydrothermal approach. Ko et al. [29] have produced nanoforests of high density, comprising long branched tree-like hierarchical crystalline ZnO nanowires. In order to improve the synthesis efficiency, the two-step strategy was developed by using seeded substrate where the primary low dimensional structures were formed, followed by a further chemical reaction process to obtain the final hierarchical structures. For example, Xu et al. [32] reported a two-step synthesis process to prepare hierarchical ZnO nanowire-nanosheet arrays that referred to two processes: (1) the preparation of ZnO nanosheet arrays on conductive glass substrates; and (2) the aqueous chemical growth of ZnO nanowires on the surfaces of the primary ZnO nanosheets (Figure 2). Cheng et al. [33] produced branched ZnO nanowires on conductive glass substrates via a similar strategy. Such hierarchical ZnO nanostructures can also be produced on other substrates, such as ITO, FTO, silicon, etc. [34–37].

Despite multi-step self-assembly with multi-discontinuous processes having been widely used in the fabrication of hierarchical ZnO structures, problems such as long reaction times and tedious procedures could limit the application for large-scale production. To deal with such problems, multi-step self-assembly completed in one-pot solution synthesis has been developed for efficient fabrication of hierarchical ZnO nanostructures. Using such a strategy, Lu et al. [38] reported a two-step continuous approach in one-pot reaction to construct ZnO 3D superstructures, in which the crystallization and the assembly process were controlled by a steady gas/liquid between H₂O₂ and dimethylsulfoxide (DMSO) organic solvent. The first step was the assembling of microspheres from ZnO nanorod building blocks, followed by the formation of the 3D superstructure via the connection within those microspheres' units side-by-side in a secondary assembly process. In other cases, hierarchical ZnO nanostructures composed of ZnO nanosheets [39] or ZnO nanorods [40] could also be obtained.

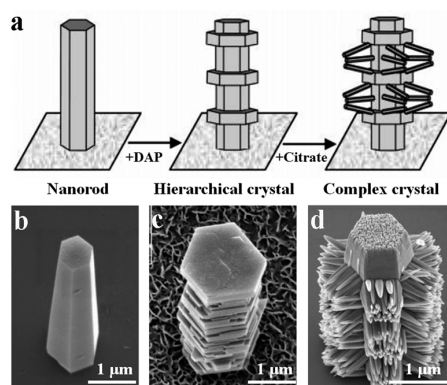


Figure 1. (a) Schematic illustration of the formation of ZnO complex crystals. (b–d) SEM images of samples at different formation steps (Reproduced with permission from [30], Copyright 2006, American Chemical Society).

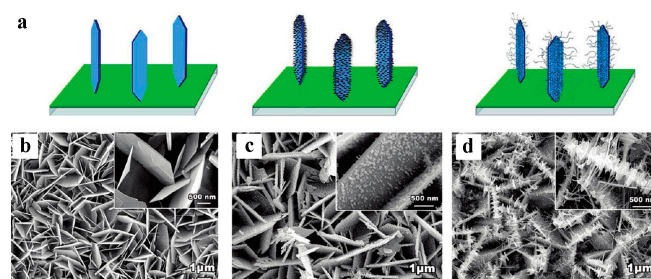


Figure 2. (a) The schematic process of the hierarchical ZnO nanoarchitectures and (b–d) SEM images of the hierarchical ZnO nanowire-nanosheet architectures at different stages (Reproduced with permission from [32], Copyright 2010, American Chemical Society).

Recently, we reported hierarchical ZnO architectures assembled by nanosheets and nanorods via a facile solution method [41]. In this reaction system, the critical morphology controller is the concentration of OH^- . When OH^- was contained at 0.33 mol/L, the ZnO nanosheets were first formed as the substrates for the heterogeneous nucleation and growth, and then, ZnO nanorod arrays that were oriented grew on the nanosheets in a secondary assembly process to generate the ZnO nanosheet-nanorod structures in which $\gamma\text{-Zn}(\text{OH})_2$ and $\epsilon\text{-Zn}(\text{OH})_2$ acted as the zinc sources for the growth of nanorod arrays (Figure 3). The above developed approaches allowed the stepwise control of experimental conditions and provided an opportunity for the rational design and synthesis of controlled architectures in nanostructures.

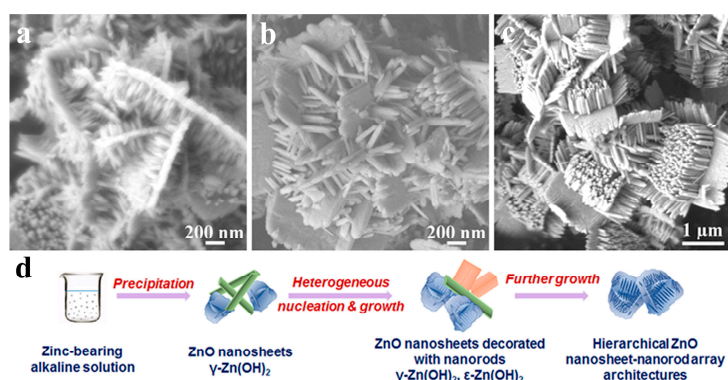


Figure 3. (a–c) Morphology evolution of products. (d) Schematic illustration for the metastable phase-directed formation mechanism of hierarchical ZnO nanosheets-nanorods (Reproduced with permission from [41], Copyright 2016, American Chemical Society).

3.2. Template-Based Synthesis

Template-based syntheses were most widely used in fabricating hollow structures, porous structures, bio-inspired structures, etc., due to the advantages of well-controlled morphology, large-scale production and diverse templates [42]. Generally, the formation process involves the growth of desired materials on hard templates, such as polymer, silica and carbon, which can be removed by chemical etching or thermal decomposition, or soft templates, such as emulsion micelles and even bubbles [43–49].

3.2.1. Hierarchical ZnO Hollow Structures

The ZnO hollow structures can be constructed in many forms, such as various hollow spheres, including core-shell, yolk-shell and some other interesting morphologies. For example, Dilger et al. [50] reported yolk-shell and hollow ZnO spheres synthesized by gas phase treatment at different temperatures in which the SiO₂ hard templates could be partially or fully removed. Soft templates can also be selected to assist the formation of hollow structures. Sinha et al. [25] reported that ZnO hollow spheroids could be obtained by using a soft template as water bubbles via a modified hydrothermal method under tungsten light irradiation. In addition, a co-surfactant template, including a triblock copolymer of complex polyethylene oxide-poly-propylene oxide-polyethylene oxide (PEO₂₀-PPO₇₀-PEO₂₀, P₁₂₃) and absolute ethanol (EtOH), was employed to assist the formation of ZnO hollow spheres by Sun et al. [51]. In another case, Yin et al. [52] proposed a water-soluble biopolymer as soft templates used in producing hollow cage-like superstructures assembled by ZnO nanorods constructed with, and the number of the hollow cages could be adjusted by verifying the reaction time. Typically, the morphology of ZnO double-cage structures is as shown in Figure 4.

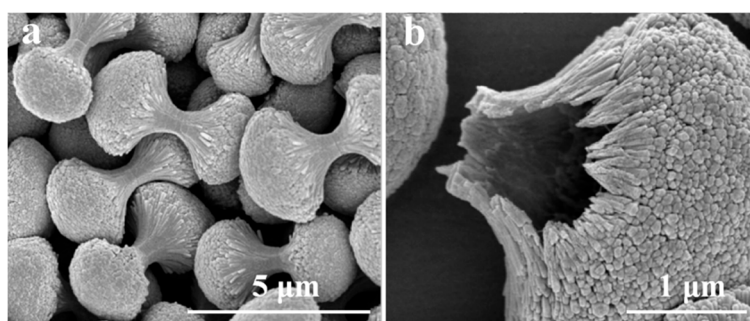


Figure 4. (a) SEM images of the double-cage nanorod-assembled ZnO structures and (b) several broken superstructures confirming that these kinds of structures are hollow (Reproduced with permission from [52], Copyright 2010, American Chemical Society).

3.2.2. Porous Hierarchical ZnO Nanostructures

Owing to the large active surface areas favoring the diffusion of guest molecules, porous structures have attracted increasing attention, especially the three-dimensionally-ordered macroporous (3DOM) nanostructures [53]. Wang et al. [54] synthesized In-doped ZnO 3DOM structures using PMMA microspheres as templates through a one-step colloidal crystal templating (CCT) approach (Figure 5). The PMMA hard templates could be easily removed by calcination. In another case, ZnO 3DOM structures were synthesized directly inside the microreactor using opals as the template [55]. The opals were first self-assembled on the channels of the microreactor to generate channels for the Zn source and finally removed by calcination. A similar synthesis strategy was also used to fabricate other ZnO porous structures, such as C-doped ZnO hierarchical structures on an ITO substrate [26]. In addition, through a one-step CCT route, Kim et al. [56] reported surfactant-templated methods to prepare hierarchical ZnO mesoporous structures from a coupling reaction of lauroyl chloride with different amino acids.

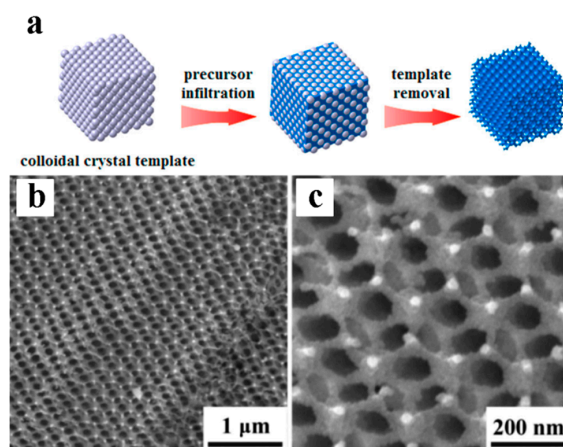


Figure 5. Schematic illustration of the experimental procedure (a) and SEM images of the three-dimensionally-ordered macroporous (3DOM) In-ZnO structures (b,c) (Reproduced with permission from [54], Copyright 2016, American Chemical Society).

3.2.3. Bio-Inspired ZnO Hierarchical Structures

Inspired by nature, researchers have developed biomimetic routes to fabricate some interesting artificial structures with certain functions. Using butterfly wings as templates, a biomorphic ZnO replica with hierarchical periodic raster structures was synthesized under a three-step process [57]. Instead of using biological templates, biomimetic ZnO plate twin-crystal periodical arrays were deposited on a patterned substrate that was gelatin assisted under mild conditions [58]. Yin et al. [59] reported a bio-inspired photoelectrode of a ZnO-modified graphene honeycomb film fabricated by a two-step process involving self-assembly of graphene oxide/dimethyldioctadecylammonium (GO/DODA), followed by reduction of GO and in situ growth of ZnO nanorods under hydrothermal treatment. Sun et al. [60] described fish-scale bio-inspired multifunctional ZnO nanostructures that have a similar morphology and structure to the cycloid scales of the Asian Arowana using templates such as PEO₂₀-PPO₇₀-PEO₂₀, P123 and EG co-surfactant. A similar strategy was used for rhabdom-like ZnO microspheres bio-inspired by fly eyes [61].

Besides, layer-layer architectural [62], binding peptides [63], flowerlike, spindle-like, sword-like, umbellar-like, prism-like [64,65], biprisms-like [66] and other interesting hierarchical structures [67] can also be fabricated under template-based routes.

3.3. Template-Free Self-Organization

Template-based methods have been widely used in the fabrication of hierarchical ZnO structures. However, some typical disadvantages, such as a long reaction process, the high cost of templates, some uncontrollable morphological changes during template removal and the presence of heterogeneous impurities, remain [3]. To deal with those drawbacks, hence, convenient and efficient routes such as template-free methods have been developed for the fabrication of hierarchical nanostructures [68,69]. Among them, template-free self-organization is one of the most simple and effective routes to fabricate various hierarchical ZnO structures.

One of the most effective ways to fabricate a ZnO hollow structure is the Ostwald ripening process (ORP), which involves the coarsening of smaller particles into bigger particles [70,71]. Wang and his co-workers produced hollow ZnO microspheres via a one-pot template-free hydrothermal synthesis and found that the hollowness of these microspheres could be controlled by adjusting the zinc source concentration [72] (Figure 6). Ji et al. [73] reported hierarchical nanostructured ZnO dandelion-like hollow spheres synthesized by a one-step solvothermal method. Using a similar route, hierarchical ZnO hollow spheres consisting of nanoparticles were prepared by a microwave-assisted solvothermal method [74].

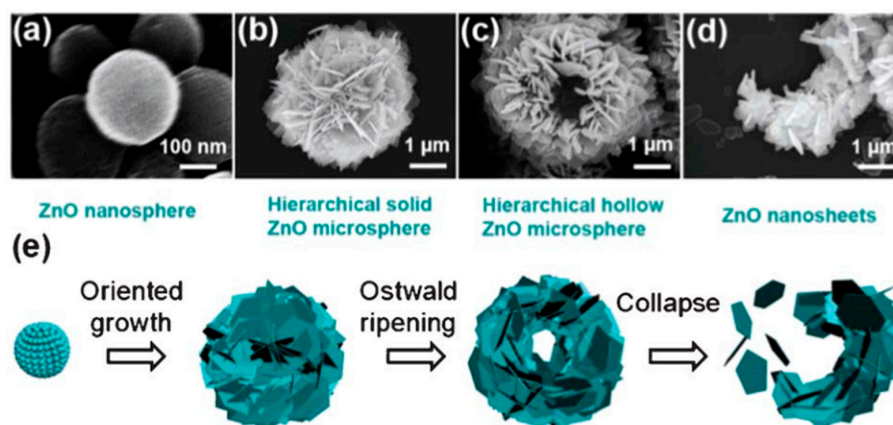


Figure 6. SEM images of the morphology evolution at different reaction times (a–d). (e) Schematic illustration of the formation process of the hierarchical hollow ZnO structure (Reproduced with permission from [72]. Copyright 2013, Royal Society of Chemistry).

The self-organization strategy can be also used to fabricate ZnO hierarchical structures assembled by tunable building blocks. For example, ZnO hierarchical structures composed of interconnected and monocrystalline nanosheets can be constructed in an aqueous solution system without any templates under sonochemical treatment at room temperature [75]. The formation of the hierarchical structures is based on oriented attachment and reconstruction. In the reaction synthesis system, thicker, porous and coarse crystallized ZnO sheets were first constructed via oriented attachment of small-sized nanocrystals. After reconstruction, ultrathin, integrated and monocrystalline nanosheets were obtained (Figure 7). Based on the policy, various hierarchical ZnO structures, such as flower-like [76–78], comb-like [79], pompon-like [80], nanocrystallite aggregates [81], twin-sphere [82], hyperbranched array [83], hexagonal-pyramid-like microcrystals [84,85], etc., could also be obtained. Pachauri et al. [86] demonstrated various hierarchical structures, including flower-like, viscous-fingers-like and rolling-pin-like, using nanoplatelets as basic building blocks and Yagi-Uda-antenna-like ZnO hierarchical structures deploying nanowires as building blocks obtained under a simple low-temperature chemical bath-based growth procedure. The morphology of such hierarchical structures could be adjusted by the regulation of the precursors.

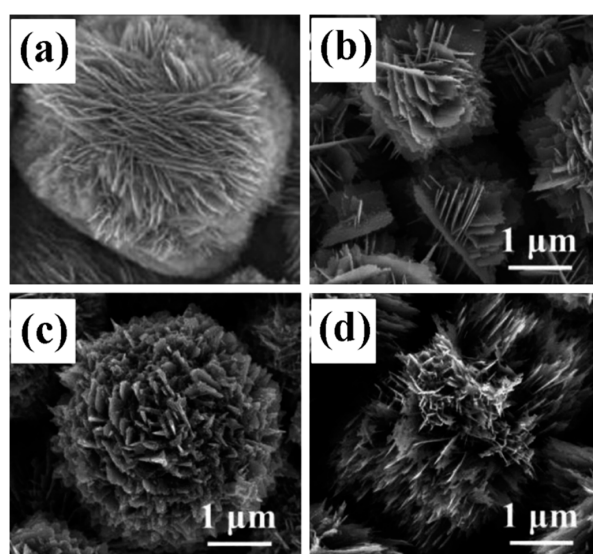


Figure 7. SEM images of different hierarchical ZnO structures. (a–d) (Reproduced with permission from [75], Copyright 2013, American Chemical Society).

Controllable hierarchical structures can also be prepared by regulating the pH [87] or the concentration of precursors [88]. Recently, we reported the ultra-rapid formation of various hierarchical ZnO structures, such as nanorods-based micro flowers, nanosheet-based microspheres and nanoparticles in star-like assemblies, via a facile solution method [89]. The shape of the nanoscale building blocks of the hierarchical structures could be easily controlled by adjusting the supersaturation depending on the variation of dilution ratios or the $[\text{OH}^-]$ to $[\text{Zn}^{2+}]$ ratios. With the increasing of supersaturation from 1.26, to 2.34, to 3.51, the morphology of hierarchical ZnO nanostructures transformed from nanorods-based to nanosheets-based and, finally, to nanoparticle-based assemblies, and the formation time of hierarchical ZnO structures decreased from 2 h to 30 s (Figure 8). Owing to the superiorities of template-free methods, further efforts should be made to achieve the large-scale synthesis of various hierarchical structures.

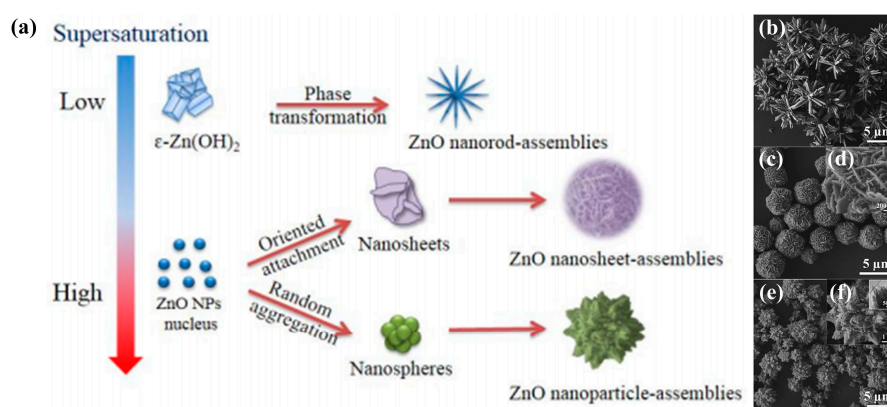


Figure 8. Schematic illustration for the formation mechanisms of ZnO hierarchical structures (a) and different SEM images of different morphologies of hierarchical ZnO nanostructures (b–f) (Reproduced with permission from [89]. Copyright 2014, Royal Society of Chemistry, London).

3.4. Precursor or Self-Templating Strategies

Another typical template-free route is the so-called precursor-derived or self-templating route. The synthesis process is followed by two main steps including the formation of precursors containing specific hierarchical structures followed by the calcination of the precursors to obtain the final products. The precursors used to prepare hierarchical structures are usually classified into inorganic and organic precursors.

Zinc-containing inorganic salts with a specific hierarchical morphology were usually selected to synthesize various hierarchical ZnO nanostructures. For instance, using a layered basic zinc carbonate (LBZC)-containing multi-layered structure as the precursor, mesoporous hierarchical ZnO nanostructures can be obtained as annealing products keeping the morphology, shape and sizes of the precursor LBZC [21]. Since the morphology of materials depends on the selection of precursors, many researchers focused on the facile formation of precursors. Liu et al. [90] introduced a PEG-mediated organic-inorganic interface cooperative self-organization strategy applied to achieve the self-assembly of $\text{Zn}_5(\text{CO}_3)_2(\text{OH})_6$ nanosheets into flower-like 3D superstructures, then the 3D structures composed of nanosheets transformed into porous ZnO nanosheet-based hierarchical structures without morphology change. Furthermore, using the same precursors, Sinhamahapatra et al. [91] reported 3D hierarchically-porous ZnO architectures constructed of two-dimensional (2D) nanosheets through the calcination of the hydrozincite intermediate. Such flower-like ZnO hierarchical structures were also obtained by using $\text{Zn}_4(\text{OH})_6\text{SO}_4 \cdot 4\text{H}_2\text{O}$ as the precursor [92]. For another different morphology of ZnO hierarchical structures, Wang et al. [93] prepared nest-like 3D ZnO porous structures through annealing the zinc hydroxide carbonate precursor, which was obtained by a one-pot hydrothermal process (Figure 9). A three-dimensional hierarchical porous ZnO with a tubular structure has been prepared

by calcining a tubular hierarchical hydrozincite precursor [94]. A bladed bundle-like architecture has been fabricated from many precursors, such as $\text{ZnO} \cdot 0.33\text{ZnBr}_2 \cdot 1.74\text{H}_2\text{O}$, zinc glycerol and Zn-based hydroxide double salts (Zn-HDS) [95–98].

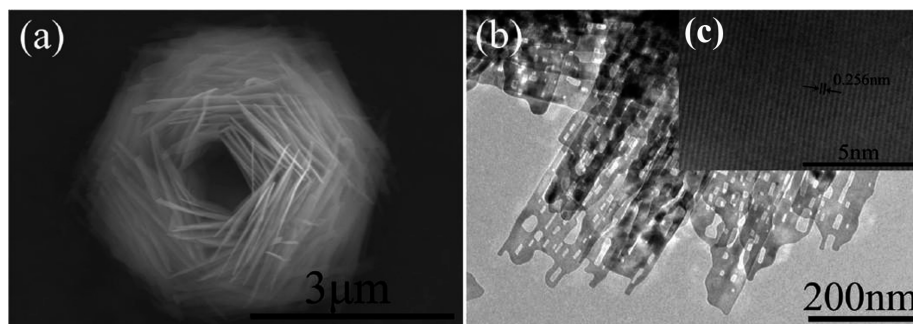


Figure 9. (a) SEM, (b) TEM and (c) HR-TEM images of nest-like 3D ZnO porous structures (Reproduced with permission from [93], Copyright 2014, American Chemical Society).

Besides those mentioned ZnO hierarchical structures formed from inorganic zincite-based salts, some organic zinc-bearing precursors were also employed. For example, Hong et al. [97] demonstrated a facile approach to prepare sheet-like hierarchical ZnO structures by treating zinc glycerol precursor with a calcination process. Moreover, Yang et al. prepared hierarchical aggregates of ZnO nanoparticles with 3D cubic morphologies via simple heat treatment of MOF-5 under different atmospheric conditions [20]. Furthermore, from the decomposition of the MOF-5 precursor, Li et al. reported hierarchical ZnO parallelepiped [99]. Thus, it is desirable to obtain more and more interesting hierarchical structures via precursor or self-templating strategies in future research.

4. Fabrication of Hierarchical ZnO-Based Nanocomposites

To improve the photocatalytic efficiency of ZnO, hierarchical ZnO-based composites have been widely developed by combining semiconductors, metals and carbon materials with ZnO owing to the synergistic effects between the components.

One efficient way to improve the photocatalytic activity of hierarchical ZnO nanostructures is constructing ZnO-based composites with either wide band or narrow band semiconductors. Combining this with the former could efficiently prolong the life span of photoexcited electron-hole pairs and enhance the anti-photocorrosion ability, owing to the synergistic contribution of each unit in the composites [100–102]. For example, Xiao et al. [103] prepared branched hierarchical ZnO nanorod-TiO₂ nanotube array heterostructures (ZnO NRs/NP-TNTAs) via a two-step assembly method. Compared with ZnO nanorods, the enhanced separation efficiency of the photogenerated electron-hole charge of ZnO NRs/NP-TNTAs was confirmed under photoelectrochemical studies, which led to the enhancement of RhB degradation performance. Various combinations of wide band semiconductors, such as a TiO₂ nanobelt/ZnO nanorod hierarchical nanostructure [104], branched hierarchical TiO₂/ZnO hierarchical nanostructures [105], ZnO-SnO₂ hollow spheres [106] and SnO₂-ZnO hierarchical structures with SnO₂ back bones and ZnO branches [107] (Figure 10), were developed, which all showed an enhanced photocatalytic property. Despite a certain improvement having been achieved by combining ZnO with other wide band semiconductors, problem such as low efficiency of visible-light absorption for such semiconductors, remain. Hence, to improve the overall energy conversion, narrow band semiconductors were introduced to combine with ZnO hierarchical structures. For, example, Liu et al. [108] reported nanotree-like CdS/ZnO hierarchical composites, where the ZnO nanoseeds were first coated on the surface of CdS via a surface adsorption process, and then, ZnO nanowires were grown on CdS to form the branched assemblies after a reflux process. Under irradiation of visible light, The CdS/ZnO hierarchical composites exhibited enhanced photocatalytic ability compared with both ZnO and CdS nanowires.

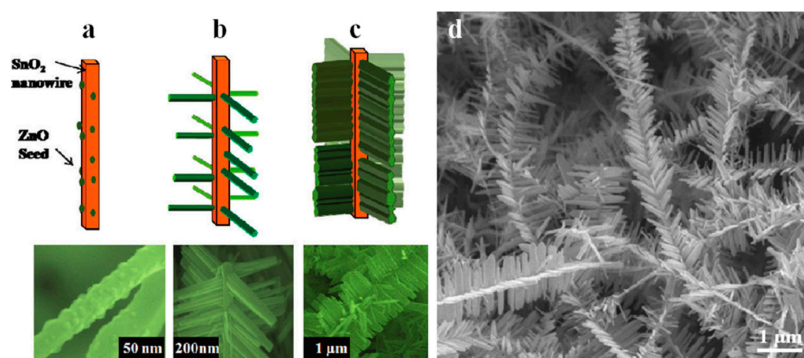


Figure 10. (a–c) Growth process of the SnO₂/ZnO hierarchical nanostructures. Top row: schematics. Bottom row: corresponding SEM images of the product. (d) SEM image of the SnO₂/ZnO hierarchical nanostructures (Reproduced with permission from [107], Copyright 2009, American Chemical Society).

Noble metals are also promised to be combined with ZnO hierarchical structures to achieve photocatalytic functionality improvements due to noble metals being able to act as electron-scavenging centers to allow for effective electron-hole pair separation [109,110]. Ahmad et al. [111] synthesized hierarchical flower-like ZnO-Au nanostructures where Au was deposited on ZnO via an electrochemical method. Nanoplate-built ZnO hollow microspheres decorated with Au nanoparticles with enhanced photocatalytic activity were produced by Xia et al. [112] through a facile solvothermal route.

Besides those mentioned, recently, carbon-based materials, such as reduced graphene oxide (rGO) and carbon nanotube (CNT), have been utilized in conjunction with ZnO hierarchical structures owing to their good conductivity and large surface area. For instance, to enhance the photocurrent and photocatalytic activity, Luo et al. [113] reported rGO-hierarchical ZnO hollow sphere composites through a 15-min ultrasonic treatment in which the conjunction between rGO and ZnO could be attributed to electronic interaction between the components. Zhang et al. [114] have prepared a ZnO-CNT heterostructure via a hydrothermal route. ZnO nanowires were grown on modified well-aligned carbon nanotube (CNT) arrays where the pre-deposited ZnO grains on the CNTs served as the nucleation sites for the growth of the ZnO nanowires. Thus, it is expected to develop more efficient and eco-friendly methods to fabricate hierarchical ZnO-based composites in the future.

5. Photocatalytic Applications of Hierarchical ZnO Nanostructures and Nanocomposites

ZnO has received much attention in many fields of photocatalysis application, such as the degradation and environmental pollutants and H₂ generation, owing to its lower cost, non-toxic and efficient photoelectrocatalytic performance [115–122]. Since ZnO (3.37 eV) has almost the same band gap energy as TiO₂ (3.2 eV), its photocatalytic capability is anticipated to be similar to that of TiO₂. Moreover, ZnO is relatively less expensive compared to TiO₂, whereby the usage of TiO₂ is uneconomical for photocatalytic application [123].

The simplified photocatalysis degradation or process of semiconductors, such as ZnO, is as follows: (1) excitation of ZnO by UV irradiation; (2) generation of excitons; (3) formation of various reactive oxidative species (ROs); and (4) oxidation of the organic compounds or reduction of the water by ROs [124–126]. H₂ generation is a photoelectrochemical process in which water can be split. However, the wide band gap ZnO (3.37 eV) could be only activated in the ultraviolet (UV) region, which accounts for less than 5% of the total energy of the solar spectrum [127,128]. Moreover, the rapid recombination of photogenerated electron-hole pairs in ZnO often leads to decreased photocatalytic activity [129]. Therefore, various elements, such as N and C, have been doped into the wide-band-gap ZnO hierarchical structures to enhance the solar energy utilization [130]. For example, N- and C-doped ZnO hierarchical photocatalysts have been found to exhibit better absorption of light in both visible and ultraviolet regions due to their smaller band gaps [130].

Especially, Liu et al. [90] reported hierarchical flower-like C-doped ZnO superstructures (ZnO flowers) assembled from porous nanosheets, which showed better photocatalytic decomposition of the RhB dye in aqueous solutions than ZnO due to the enhanced light absorption over a wide range of wavelengths. Semiconductors, such as CdS, are usually combined with ZnO to form hierarchical heterostructures for visible light photocatalytic degradation due to their narrow band gaps [108,131–133]. For example, nanoscale tree-like CdS/ZnO nanocomposites with a hierarchical architecture showed the ability for selective oxidation of thioanisole and anaerobic reduction of nitro compound 4-nitroaniline under irradiation of artificial solar light [108]. In addition, hierarchical CdS-decorated 1D ZnO nanorod-2D graphene hybrids exhibit enhanced photocatalytic activity and recycling performance toward selective reduction process under visible light irradiation [29]. In the other case, we recently reported a highly efficient direct Z-scheme Ag_3PO_4 -ZnO hierarchical photocatalysis by depositing Ag_3PO_4 particles on defect-rich ZnO hierarchical nanosheets used for degeneration of RhB under visible light irradiation [19]. The prepared heterostructured Ag_3PO_4 -ZnO samples showed higher visible light photocatalytic activity than single-phase ZnO or Ag_3PO_4 photocatalysts, which was attributed to the efficient charge transfer between ZnO and Ag_3PO_4 through a synergistic effect of surface oxygen vacancies and Ag_3PO_4 coupling. Recently, many researchers have focused on the localized surface plasmon resonance (LSPR) effect of metal nanoparticles (NPs) for visible-light-driven plasmonic photocatalysts application [134–141]. For instance, sandwiched $\text{ZnO@Au@Cu}_2\text{O}$ nanorod films were synthesized on steel mesh substrates via a simple three-step approach and showed an efficient visible-light photocatalytic performance for the degradation of the MO solution [142].

Those non-doped ZnO hierarchical composites could also be used in the field of H_2 generation [118,122,143–150]. Barpuzary et al. [143] prepared urchin-like CdS@ZnO hetero-arrays via a template-based method. The core-shell CdS@ZnO nano-urchins showed enhanced hydrogen generation with apparent quantum yields of 15% (Figure 11). Yu and his co-workers [147] fabricated a ternary heterostructure of CdS/Au/ZnO , through a two-step self-assembly process. The heterostructure of CdS/Au/ZnO showed improved photocatalytic hydrogen evolution rate with 60.8 mmol h^{-1} , which was 4.5-times higher than the CdS/ZnO heterostructure. Furthermore, Hsu et al. [146] reported that a hierarchical Ag_2S -coupled ZnO@ZnS core-shell nanorod-decorated metal wire mesh showed higher H_2 production rates reaching 5870 and $168 \mu\text{mol g}^{-1} \text{ h}^{-1}$ under UV and visible light irradiation than ZnO/metal mesh. Thus, the fabrication of hierarchical ZnO-based heterostructures is a promising strategy to enhance both photocatalytic degradation and H_2 generation.

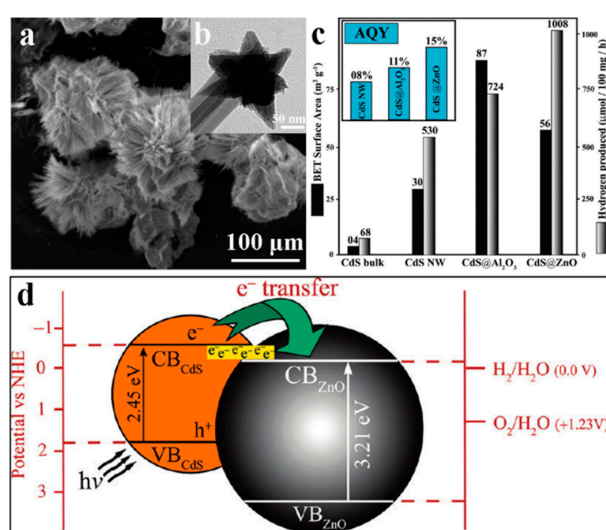


Figure 11. (a,b) SEM and TEM morphology of CdS@ZnO nano-urchins; (c) BET surface area plot and amounts of H_2 generated from different samples. (Inset) Percentage of apparent quantum yields for different samples; (d) schematic illustration for electron transfer in the CdS@ZnO nano-urchin (Reproduced with permission from [143], Copyright 2012, American Chemical Society).

6. Conclusions and Outlook

In this review, we comprehensively discussed the recent development in the synthesis routes of hierarchical ZnO nanostructures, as well as their photocatalytic potentiality. A variety of tailored hierarchical nanostructures were studied by researchers with logical design of experiment procedures. Especially, rational establishment of facile template-free synthesis technologies could be highly efficient and environmentally benign for the construction of hierarchical ZnO-based nanostructures. In addition, as photocatalysts, hierarchical ZnO-based composites combined with narrow band semiconductors or noble metals exhibited enhanced photocatalytic performance under visible light irradiation owing to their superiorities of high surface area, porosity and the synergisms among them, which led to the improvement of light utilization and charge-transfer properties. Therefore, such composites efficiently obtained under a proper template-free approach play important roles in environment and energy applications.

Although many significant achievements have been made in the synthesis of hierarchical ZnO-based nanostructures, further efforts are required to solve problems, such as small-scale, low-yield production of hierarchical ZnO-based materials, the unclear interaction mechanisms between building units and the low solar light utilization. In the future, the green, cost-effective and industry-scale template-free synthesis of hierarchical ZnO-based photocatalysts would be highly desirable. Furthermore, besides photocatalysis applications, the development of the novel syntheses of hierarchical ZnO nanostructures is also expected to lead to multiple potential applications in the fields of sensors, solar cells, electronic or photoelectrochemical devices.

Acknowledgments: This work was financially supported by the National Science Foundation of China (Nos. 51234003 and 51374138) and the National Key Technology Research and Development Program of China (2013BAC14B02).

Author Contributions: Yi Xia wrote this paper; Jing Wang, Dali Zhou and Lan Xiang worked on the concept and the revision of final version of manuscript; Ruosong Chen reproduced the figures.

Conflicts of Interest: The authors declare no conflict of interest.

References

1. Fujishima, A. Electrochemical Photolysis of Water at a Semiconductor Electrode. *Nature* **1972**, *238*, 37–38. [[CrossRef](#)] [[PubMed](#)]
2. Li, X.; Yu, J.; Low, J.; Fang, Y.; Xiao, J.; Chen, X. Engineering heterogeneous semiconductors for solar water splitting. *J. Mater. Chem. A* **2015**, *3*, 2485–2534. [[CrossRef](#)]
3. Miseki, A.K.; Miseki, Y. Heterogeneous photocatalyst materials for water splitting. *Chem. Soc. Rev.* **2009**, *38*, 253–278.
4. Li, X.; Yu, J.; Jaroniec, M. Hierarchical photocatalysts. *Chem. Soc. Rev.* **2016**, *45*, 2603–2636. [[CrossRef](#)] [[PubMed](#)]
5. Janotti, A.; Van de Walle, C.G. Fundamentals of zinc oxide as a semiconductor. *Rep. Prog. Phys.* **2009**, *72*, 126501. [[CrossRef](#)]
6. Reynolds, D.C.; Loo, D.C.; Jogai, B. Valence-band ordering in ZnO. *Phys. Rev. B* **1999**, *60*, 2340–2344. [[CrossRef](#)]
7. Chen, Y.; Bagnall, D.M.; Koh, H.; Park, K.; Hiraga, K.; Zhu, Z.; Yao, T. Plasma assisted molecular beam epitaxy of ZnO on c-plane sapphire: Growth and characterization. *J. Appl. Phys.* **1998**, *84*, 3912. [[CrossRef](#)]
8. Maiti, S.; Pal, S.; Chattopadhyay, K.K. Recent advances in low temperature, solution processed morphology tailored ZnO nanoarchitectures for electron emission and photocatalysis applications. *CrystEngComm* **2015**, *17*, 9264–9295. [[CrossRef](#)]
9. Liu, Q.; Sun, Z.; Dou, Y.; Kim, J.H.; Dou, S.X. Two-step self-assembly of hierarchically-ordered nanostructures. *J. Mater. Chem. A* **2015**, *3*, 11688–11699. [[CrossRef](#)]
10. Saito, N.; Haneda, H. Hierarchical structures of ZnO spherical particles synthesized solvothermally. *Sci. Technol. Adv. Mater.* **2011**, *12*, 064707. [[CrossRef](#)]

11. Wang, X.; Yu, J.; Ho, C.; Hou, Y.; Fu, X. Photocatalytic Activity of a Hierarchically Macro/Mesoporous Titania. *Langmuir* **2005**, *21*, 2552–2559. [[CrossRef](#)] [[PubMed](#)]
12. Yuan, Z.Y.; Ren, T.Z.; Su, B.L. Hierarchically Mesostructured Titania Materials with an Unusual Interior Macroporous Structure. *Adv. Mater.* **2003**, *15*, 1462–1465. [[CrossRef](#)]
13. Zhang, L.; Wang, W.; Zhou, L.; Xu, H. Bi₂WO₆ Nano- and Microstructures: Shape Control and Associated Visible-Light-Driven Photocatalytic Activities. *Small* **2007**, *3*, 1618–1625. [[CrossRef](#)] [[PubMed](#)]
14. Cheng, B.; Le, Y.; Cai, W.; Yu, J. Synthesis of hierarchical Ni(OH)₂ and NiO nanosheets and their adsorption kinetics and isotherms to Congo red in water. *J. Hazard. Mater.* **2011**, *185*, 889–897. [[CrossRef](#)] [[PubMed](#)]
15. Cai, W.; Yu, J.; Jaroniec, M. Template-free synthesis of hierarchical spindle-like γ -Al₂O₃ materials and their adsorption affinity towards organic and inorganic pollutants in water. *J. Mater. Chem.* **2010**, *20*, 4587. [[CrossRef](#)]
16. Yu, X.; Yu, J.; Cheng, B.; Jaroniec, M. Synthesis of Hierarchical Flower-like AlOOH and TiO₂/AlOOH Superstructures and their Enhanced Photocatalytic Properties. *J. Phys. Chem. C* **2009**, *113*, 17527–17535. [[CrossRef](#)]
17. Guo, M.Y.; Ng, A.M.C.; Liu, F.; Djurišić, A.B.; Chan, W.K.; Su, H.; Wong, K.S. Effect of Native Defects on Photocatalytic Properties of ZnO. *J. Phys. Chem. C* **2011**, *115*, 11095–11101. [[CrossRef](#)]
18. Mukhopadhyay, S.; Das, P.P.; Maity, S.; Ghosh, P.; Devi, P.S. Solution grown ZnO rods: Synthesis, characterization and defect mediated photocatalytic activity. *Appl. Catal. B Environ.* **2015**, *165*, 128–138. [[CrossRef](#)]
19. Wang, J.; Xia, Y.; Dong, Y.; Chen, R.; Xiang, L.; Komarmaneni, S. Defect-rich ZnO nanosheets of high surface area as an efficient visible-light photocatalyst. *Appl. Catal. B Environ.* **2016**, *192*, 8–16. [[CrossRef](#)]
20. Yang, S.J.; Im, J.H.; Kim, T.; Lee, K. MOF-derived ZnO and ZnO@C composites with high photocatalytic activity and adsorption capacity. *J. Hazard. Mater.* **2011**, *186*, 376–382. [[CrossRef](#)] [[PubMed](#)]
21. Xu, L.; Li, Z.; Cai, Q.; Wang, H.; Gao, H.; Lv, W.; Liu, J. Precursor template synthesis of three-dimensional mesoporous ZnO hierarchical structures and their photocatalytic properties. *CrystEngComm* **2010**, *12*, 2166. [[CrossRef](#)]
22. Zhang, L.; Yu, J.C. A sonochemical approach to hierarchical porous titania spheres with enhanced photocatalytic activity. *Chem. Commun.* **2003**, 2078–2079. [[CrossRef](#)]
23. Hu, X.; Yu, J.C.; Gong, J.; Li, Q. Rapid Mass Production of Hierarchically Porous ZnIn₂S₄ Submicrospheres via a Microwave-Solvothermal Process. *Cryst. Growth Des.* **2007**, *7*, 2444–2448. [[CrossRef](#)]
24. Ho, W.; Yu, J.C.; Lee, S. Synthesis of hierarchical nanoporous F-doped TiO₂ spheres with visible light photocatalytic activity. *Chem. Commun.* **2006**, 1115–1117. [[CrossRef](#)] [[PubMed](#)]
25. Sinha, A.K.; Basu, M.; Pradhan, M.; Sarker, S.; Pal, T. Fabrication of Large-Scale Hierarchical ZnO Hollow Spheroids for Hydrophobicity and Photocatalysis. *Chem. Eur. J.* **2010**, *16*, 7865–7874. [[CrossRef](#)] [[PubMed](#)]
26. Lin, Y.; Hsu, Y.; Chen, Y.; Chen, L.; Chen, S.; Chen, K. Visible-light-driven photocatalytic carbon-doped porous ZnO nanoarchitectures for solar water-splitting. *Nanoscale* **2012**, *4*, 6515. [[CrossRef](#)] [[PubMed](#)]
27. Xiong, T.; Dong, F.; Wu, Z. Enhanced extrinsic absorption promotes the visible light photocatalytic activity of wide band-gap (BiO)₂CO₃ hierarchical structure. *RSC Adv.* **2014**, *4*, 56307–56312. [[CrossRef](#)]
28. Ko, S.H.; Lee, D.; Kang, H.; Nam, K.; Yeo, J.; Hong, S.; Grigoropoulos, C.P.; Sung, H. Nanoforest of Hydrothermally Grown Hierarchical ZnO Nanowires for a High Efficiency Dye-Sensitized Solar Cell. *Nano Lett.* **2011**, *11*, 666–671. [[CrossRef](#)] [[PubMed](#)]
29. Han, C.; Chen, Z.; Zhang, N.; Colmenares, J.C.; Xu, Y. Hierarchically CdS Decorated 1D ZnO Nanorods-2D Graphene Hybrids: Low Temperature Synthesis and Enhanced Photocatalytic Performance. *Adv. Funct. Mater.* **2015**, *25*, 221–229. [[CrossRef](#)]
30. Zhang, T.; Dong, W.; Keeter-Brewer, M.; Konar, S.; Njabon, R.N.; Tian, Z.R. Site-Specific Nucleation and Growth Kinetics in Hierarchical Nanosyntheses of Branched ZnO Crystallites. *J. Am. Chem. Soc.* **2006**, *128*, 10960–10968. [[CrossRef](#)] [[PubMed](#)]
31. Zhang, Y.; Xu, J.; Xiang, Q.; Li, H.; Pan, Q.; Xu, P. Brush-Like Hierarchical ZnO Nanostructures: Synthesis, Photoluminescence and Gas Sensor Properties. *J. Phys. Chem. C* **2009**, *113*, 3430–3435. [[CrossRef](#)]
32. Xu, F.; Dai, M.; Lu, Y.; Sun, L. Hierarchical ZnO Nanowire–Nanosheet Architectures for High Power Conversion Efficiency in Dye-Sensitized Solar Cells. *J. Phys. Chem. C* **2010**, *114*, 2776–2782. [[CrossRef](#)]
33. Cheng, H.; Chiu, W.; Lee, C.; Tsai, S.; Hsieh, W. Formation of Branched ZnO Nanowires from Solvothermal Method and Dye-Sensitized Solar Cells Applications. *J. Phys. Chem. C* **2008**, *112*, 16359–16364. [[CrossRef](#)]

34. Xu, F.; She, Y.; Sun, L.; Zeng, H.; Lu, Y. Enhanced photocatalytic activity of hierarchical ZnO nanoplate-nanowire architecture as environmentally safe and facily recyclable photocatalyst. *Nanoscale* **2011**, *3*, 5020–5025. [[CrossRef](#)]
35. Kim, H.; Yong, K. Highly Efficient Photoelectrochemical Hydrogen Generation Using a Quantum Dot Coupled Hierarchical ZnO Nanowires Array. *ACS Appl. Mater. Interfaces* **2013**, *5*, 13258–13264. [[CrossRef](#)] [[PubMed](#)]
36. Luo, Q.; Lei, B.; Yu, X.; Kuang, D.; Su, C. Hierarchical ZnO rod-in-tube nano-architecture arrays produced via a two-step hydrothermal and ultrasonication process. *J. Mater. Chem* **2011**, *21*, 8709–8714. [[CrossRef](#)]
37. Alenezi, M.R.; Henley, S.J.; Emerson, N.G.; Silva, S.R.P. From 1D and 2D ZnO nanostructures to 3D hierarchical structures with enhanced gas sensing properties. *Nanoscale* **2014**, *6*, 235–247. [[CrossRef](#)] [[PubMed](#)]
38. Pai, L.; Xue, D. ZnO 3D-Superstructures via Two-Step Assembly at Gas/Liquid Interface. *Nanosci. Nanotechnol. Lett.* **2011**, *3*, 429–433.
39. Guo, H.; Zhu, Q.; Wu, X.; Jiang, Y.; Xie, X.; Xu, A. Oxygen deficient ZnO_{1-x} nanosheets with high visible light photocatalytic activity. *Nanoscale* **2015**, *7*, 7216–7223. [[CrossRef](#)] [[PubMed](#)]
40. Chen, M.; Wang, Y.; Song, L.; Gunawan, P.; Zhong, Z.; She, X.; Su, F. Urchin-like ZnO microspheres synthesized by thermal decomposition of hydrozincite as a copper catalyst promoter for the Rochow reaction. *RSC Adv.* **2012**, *2*, 4164. [[CrossRef](#)]
41. Wang, J.; Li, X.; Xia, Y.; Komarneni, S.; Chen, H.; Xu, J.; Xiang, L.; Xie, D. Hierarchical ZnO Nanosheet-Nanorod Architectures for Fabrication of Poly(3-hexylthiophene)/ZnO Hybrid NO₂ Sensor. *ACS Appl. Mater. Interfaces* **2016**, *8*, 8600–8607. [[CrossRef](#)] [[PubMed](#)]
42. Liu, Y.; Goebel, J.; Yin, Y. Templated synthesis of nanostructured materials. *Chem. Soc. Rev.* **2013**, *42*, 2610–2653. [[CrossRef](#)] [[PubMed](#)]
43. Bard, A.J.; Fox, M.A. Artificial Photosynthesis: Solar Splitting of Water to Hydrogen and Oxygen. *Acc. Chem. Res.* **1995**, *28*, 141–145. [[CrossRef](#)]
44. Liu, G.; Wang, T.; Zhang, H.; Meng, X.; Hao, D.; Chang, K.; Li, P.; Kako, T.; Ye, J. Nature-Inspired Environmental “Phosphorylation” Boosts Photocatalytic H₂ Production over Carbon Nitride Nanosheets under Visible-Light Irradiation. *Angew. Chemie Int. Ed.* **2015**, *54*, 13561–13565. [[CrossRef](#)] [[PubMed](#)]
45. Wang, Z.; Luan, D.; Boey, F.; Lou, X.W. Fast Formation of SnO₂ Nanoboxes with Enhanced Lithium Storage Capability. *J. Am. Chem. Soc.* **2011**, *133*, 4738–4741. [[CrossRef](#)] [[PubMed](#)]
46. Ding, S.; Chen, J.S.; Qi, G.; Duan, X.; Wang, Z.; Giannelis, E.P.; Archer, L.A.; Lou, X.W. Formation of SnO₂ Hollow Nanospheres inside Mesoporous Silica Nanoreactors. *J. Am. Chem. Soc.* **2011**, *133*, 21–23. [[CrossRef](#)] [[PubMed](#)]
47. Yin, X.M.; Li, C.C.; Zhang, M.; Hao, Q.Y.; Liu, S.; Chen, L.B.; Wang, T.H. One-Step Synthesis of Hierarchical SnO₂ Hollow Nanostructures via Self-Assembly for High Power Lithium Ion Batteries. *J. Phys. Chem. C* **2010**, *114*, 8084–8088. [[CrossRef](#)]
48. Jiang, L.; Wu, X.; Guo, Y.; Wan, L. SnO₂-Based Hierarchical Nanomicrostructures: Facile Synthesis and Their Applications in Gas Sensors and Lithium-Ion Batteries. *J. Phys. Chem. C* **2009**, *113*, 14213–14219. [[CrossRef](#)]
49. Wang, W.; Dahl, M.; Yin, Y. Hollow Nanocrystals through the Nanoscale Kirkendall Effect. *Chem. Mater.* **2013**, *25*, 1179–1189. [[CrossRef](#)]
50. Dilger, S.; Wessig, M.; Wagner, M.; Reparaz, J.; Torres, C.; Liang, Q.; Dekorsy, T.; Polarz, S. Nanoarchitecture Effects on Persistent Room Temperature Photoconductivity and Thermal Conductivity in Ceramic Semiconductors: Mesoporous, Yolk-Shell, and Hollow ZnO Spheres. *Cryst. Growth Des.* **2014**, *14*, 4593–4601. [[CrossRef](#)]
51. Sun, Z.; Liao, T.; Liu, K.; Kim, J.H.; Dou, S.X. Robust superhydrophobicity of hierarchical ZnO hollow microspheres fabricated by two-step self-assembly. *Nano Res.* **2013**, *6*, 726–735. [[CrossRef](#)]
52. Yin, J.; Lu, Q.; Yu, Z.; Wang, J.; Pang, H.; Gao, F. Hierarchical ZnO Nanorod-Assembled Hollow Superstructures for Catalytic and Photoluminescence Applications. *Cryst. Growth Des.* **2010**, *10*, 40–43. [[CrossRef](#)]
53. Stein, A.; Li, F.; Denny, N.R. Morphological Control in Colloidal Crystal Templating of Inverse Opals, Hierarchical Structures, and Shaped Particles. *Chem. Mater.* **2008**, *20*, 649–666. [[CrossRef](#)]
54. Wang, Z.; Tian, Z.; Han, D.; Gu, F. Highly Sensitive and Selective Ethanol Sensor Fabricated with In-Doped 3DOM ZnO. *ACS Appl. Mater. Interfaces* **2016**, *8*, 5466–5474. [[CrossRef](#)] [[PubMed](#)]

55. Lin, Y.; Hsu, Y.; Chen, S.; Chen, L.; Chen, K. O₂ plasma-activated CuO-ZnO inverse opals as high-performance methanol microreformer. *J. Mater. Chem.* **2010**, *20*, 10611. [[CrossRef](#)]
56. Kim, S.H.; Olson, T.Y.; Satcher, J.H.; Han, T.Y.J. Hierarchical ZnO structures templated with amino acid based surfactants. *Microporous Mesoporous Mater.* **2012**, *151*, 64–69. [[CrossRef](#)]
57. Zhang, W.; Zhang, D.; Fan, T.; Ding, J.; Guo, Q.; Ogawa, H. Morphosynthesis of hierarchical ZnO replica using butterfly wing scales as templates. *Microporous Mesoporous Mater.* **2006**, *92*, 227–233. [[CrossRef](#)]
58. Tseng, Y.; Liu, M.; Kuo, Y.; Chen, P.; Chen, C.; Chen, Y.; Mou, C. Biomimetic ZnO plate twin-crystals periodical arrays. *Chem. Commun.* **2012**, *48*, 3215. [[CrossRef](#)] [[PubMed](#)]
59. Yin, S.; Men, X.; Sun, H.; She, P.; Zhang, W.; Wu, C.; Qin, W.; Chen, X. Enhanced photocurrent generation of bio-inspired graphene/ZnO composite films. *J. Mater. Chem. A* **2015**, *3*, 12016–12022. [[CrossRef](#)]
60. Sun, Z.; Liao, T.; Li, W.; Dou, Y.; Liu, K.; Jiang, L.; Kim, S.; Kim, J.; Dou, S. Fish-scale bio-inspired multifunctional ZnO nanostructures. *NPG Asia Mater.* **2015**, *7*, e232. [[CrossRef](#)]
61. Sun, Z.; Liao, T.; Liu, K.; Jiang, L.; Kim, J.H.; Dou, S.X. Fly-Eye Inspired Superhydrophobic Anti-Fogging Inorganic Nanostructures. *Small* **2014**, *10*, 3001–3006. [[CrossRef](#)] [[PubMed](#)]
62. Li, C.C.; Yin, X.M.; Li, Q.H.; Wang, T.H. Enhanced gas sensing properties of ZnO/SnO₂ hierarchical architectures by glucose-induced attachment. *CrystEngComm* **2011**, *13*, 1557–1563. [[CrossRef](#)]
63. Limo, M.J.; Ramasamy, R.; Perry, C.C. ZnO Binding Peptides: Smart Versatile Tools for Controlled Modification of ZnO Growth Mechanism and Morphology. *Chem. Mater.* **2015**, *27*, 1950–1960. [[CrossRef](#)]
64. Wang, X.; Zhang, Q.; Wan, Q.; Dai, G.; Zhou, C.; Zou, B. Controllable ZnO Architectures by Ethanolamine-Assisted Hydrothermal Reaction for Enhanced Photocatalytic Activity. *J. Phys. Chem. C* **2011**, *115*, 2769–2775. [[CrossRef](#)]
65. Wu, Q.; Chen, X.; Zhang, P.; Han, Y.; Chen, X.; Yan, Y.; Li, S. Amino Acid-Assisted Synthesis of ZnO Hierarchical Architectures and Their Novel Photocatalytic Activities. *Cryst. Growth Des.* **2008**, *8*, 3010–3018. [[CrossRef](#)]
66. Zhang, X.L.; Qiao, R.; Qiu, R.; Kim, J.C.; Kang, Y.S. Fabrication of Hierarchical ZnO Nanostructures via a Surfactant-Directed Process. *Cryst. Growth Des.* **2009**, *9*, 2906–2910. [[CrossRef](#)]
67. Stan, A.; Munteanu, C.; Musuc, A.; Birjega, R.; Ene, R.; Ianculescu, A.; Raut, I.; Jecu, L.; Doni, M.; Anghel, E.; et al. A general, eco-friendly synthesis procedure of self-assembled ZnO-based materials with multifunctional properties. *Dalton Trans.* **2015**, *44*, 7844–7853. [[CrossRef](#)] [[PubMed](#)]
68. Yan, S.C.; Ouyang, S.X.; Gao, J.; Yang, M.; Feng, J.; Fan, X.; Wan, L.; Sheng, Z.; Ye, J.H.; Zhou, Y.; et al. A Room-Temperature Reactive-Template Route to Mesoporous ZnGa₂O₄ with Improved Photocatalytic Activity in Reduction of CO₂. *Angew. Chemie Int. Ed.* **2010**, *49*, 6400–6404. [[CrossRef](#)] [[PubMed](#)]
69. Zhang, Q.; Wang, W.; Geobl, J.; Yin, Y. Self-templated synthesis of hollow nanostructures. *Nano Today* **2009**, *4*, 494–507. [[CrossRef](#)]
70. Zeng, H.C. Synthetic architecture of interior space for inorganic nanostructures. *J. Mater. Chem.* **2006**, *16*, 649–662. [[CrossRef](#)]
71. Wang, H.; Rogach, A.L. Hierarchical SnO₂ Nanostructures: Recent Advances in Design, Synthesis, and Applications. *Chem. Mater.* **2014**, *26*, 123–133. [[CrossRef](#)]
72. Wang, D.; Du, S.; Zhou, X.; Wang, B.; Ma, J.; Sun, P.; Sun, Y.; Lu, G. Template-free synthesis and gas sensing properties of hierarchical hollow ZnO microspheres. *CrystEngComm* **2013**, *15*, 7438. [[CrossRef](#)]
73. Jia, Q.; Ji, H.; Zhang, Y.; Chen, Y.; Sun, X.; Jin, Z. Rapid and selective detection of acetone using hierarchical ZnO gas sensor for hazardous odor markers application. *J. Hazard. Mater.* **2014**, *276*, 262–270. [[CrossRef](#)] [[PubMed](#)]
74. Zhao, X.; Qi, L. Rapid microwave-assisted synthesis of hierarchical ZnO hollow spheres and their application in Cr(VI) removal. *Nanotechnology* **2012**, *23*, 235604. [[CrossRef](#)] [[PubMed](#)]
75. Shi, Y.; Zhu, C.; Wang, L.; Zhao, C.; Li, W.; Fung, K.; Ma, T.; Hagfeldt, A.; Wang, N. Ultrarapid Sonochemical Synthesis of ZnO Hierarchical Structures: From Fundamental Research to High Efficiencies up to 6.42% for Quasi-Solid Dye-Sensitized Solar Cells. *Chem. Mater.* **2013**, *25*, 1000–1012. [[CrossRef](#)]
76. Cai, Y.; Fan, H. One-step self-assembly economical synthesis of hierarchical ZnO nanocrystals and their gas-sensing properties. *CrystEngComm* **2013**, *15*, 9148–9153. [[CrossRef](#)]
77. Shi, Y.; Zhu, C.; Wang, L.; Li, W.; Cheng, C.; Ho, K.; Fung, K.; Wang, N. Optimizing nanosheet-based ZnO hierarchical structure through ultrasonic-assisted precipitation for remarkable photovoltaic enhancement in quasi-solid dye-sensitized solar cells. *J. Mater. Chem.* **2012**, *22*, 13097. [[CrossRef](#)]

78. Krishnapriya, R.; Praneetha, S.; Murugan, A.V. Investigation of the effect of reaction parameters on the microwave-assisted hydrothermal synthesis of hierarchical jasmine-flower-like ZnO nanostructures for dye-sensitized solar cells. *New J. Chem.* **2016**, *40*, 5080–5089. [[CrossRef](#)]
79. Xu, X.; Wu, M.; Asoro, M.; Ferreira, P.J.; Fan, D.L. One-Step Hydrothermal Synthesis of Comb-Like ZnO Nanostructures. *Cryst. Growth Des.* **2012**, *12*, 4829–4833. [[CrossRef](#)] [[PubMed](#)]
80. Xu, F.; Guo, D.; Han, H.; Wang, H.; Gao, Z.; Wu, D.; Jiang, K. Room-temperature synthesis of pompon-like ZnO hierarchical structures and their enhanced photocatalytic properties. *Res. Chem. Intermed.* **2012**, *38*, 1579–1589. [[CrossRef](#)]
81. Gao, R.; Liang, Z.; Tian, J.; Zhang, Q.; Wang, L.; Cao, G. ZnO nanocrystallite aggregates synthesized through interface precipitation for dye-sensitized solar cells. *Nano Energy* **2013**, *2*, 40–48. [[CrossRef](#)]
82. Li, F.; Gong, F.; Xiao, Y.; Zhang, A.; Zhao, J.; Fang, S.; Jia, D. ZnO Twin-Spheres Exposed in $\pm(001)$ Facets: Stepwise Self-Assembly Growth and Anisotropic Blue Emission. *ACS Nano* **2013**, *7*, 10482–10491. [[CrossRef](#)] [[PubMed](#)]
83. Wu, W.; Feng, H.; Rao, H.; Xu, Y.; Kuang, D.; Su, C. Maximizing omnidirectional light harvesting in metal oxide hyperbranched array architectures. *Nat. Commun.* **2014**, *5*, 3968. [[CrossRef](#)] [[PubMed](#)]
84. Yang, M.; Sun, K.; Kotov, N.A. Formation and Assembly–Disassembly Processes of ZnO Hexagonal Pyramids Driven by Dipolar and Excluded Volume Interactions. *J. Am. Chem. Soc.* **2010**, *132*, 1860–1872. [[CrossRef](#)] [[PubMed](#)]
85. Lu, F.; Cai, W.; Zhang, Y. ZnO Hierarchical Micro/Nanoarchitectures: Solvothermal Synthesis and Structurally Enhanced Photocatalytic Performance. *Adv. Funct. Mater.* **2008**, *18*, 1047–1056. [[CrossRef](#)]
86. Pachauri, V.; Kern, K.; Balasubramanian, K. Template-free self-assembly of hierarchical ZnO structures from nanoscale building blocks. *Chem. Phys. Lett.* **2010**, *498*, 317–322. [[CrossRef](#)]
87. Chetia, T.R.; Ansari, M.S.; Qureshi, M. Rational design of hierarchical ZnO superstructures for efficient charge transfer: Mechanistic and photovoltaic studies of hollow, mesoporous, cage-like nanostructures with compacted 1D building blocks. *Phys. Chem. Chem. Phys.* **2016**, *18*, 5344–5357. [[CrossRef](#)] [[PubMed](#)]
88. Desai, M.A.; Sartale, S.D. Facile Soft Solution Route to Engineer Hierarchical Morphologies of ZnO Nanostructures. *Cryst. Growth Des.* **2015**, *15*, 4813–4820. [[CrossRef](#)]
89. Wang, J.; Hou, S.; Zhang, L.; Chen, J.; Xiang, L. Ultra-rapid formation of ZnO hierarchical structures from dilution-induced supersaturated solutions. *CrystEngComm* **2014**, *16*, 7115. [[CrossRef](#)]
90. Liu, S.; Li, C.; Yu, J.; Xiang, Q. Improved visible-light photocatalytic activity of porous carbon self-doped ZnO nanosheet-assembled flowers. *CrystEngComm* **2011**, *13*, 2533–2541. [[CrossRef](#)]
91. Sinhamahapatra, A.; Giri, A.; Pal, P.; Pahari, S.; Bajaj, H.; Panda, A. A rapid and green synthetic approach for hierarchically assembled porous ZnO nanoflakes with enhanced catalytic activity. *J. Mater. Chem.* **2012**, *22*, 17227. [[CrossRef](#)]
92. Liang, W.; Li, W.; Chen, H.; Liu, H.; Zhu, L. Exploiting electrodeposited flower-like $\text{Zn}_4(\text{OH})_6\text{SO}_4 \cdot 4\text{H}_2\text{O}$ nanosheets as precursor for porous ZnO nanosheets. *Electrochim. Acta* **2015**, *156*, 171–178. [[CrossRef](#)]
93. Wang, X.; Liu, W.; Liu, J.; Wang, F.; Kong, J.; Qiu, S.; He, C.; Luan, L. Synthesis of Nestlike ZnO Hierarchically Porous Structures and Analysis of Their Gas Sensing Properties. *ACS Appl. Mater. Interfaces* **2012**, *4*, 817–825. [[CrossRef](#)] [[PubMed](#)]
94. Fan, F.; Tang, P.; Wang, Y.; Feng, Y.; Chen, A.; Luo, R.; Li, D. Facile synthesis and gas sensing properties of tubular hierarchical ZnO self-assembled by porous nanosheets. *Sens. Actuators B Chem.* **2015**, *215*, 231–240. [[CrossRef](#)]
95. Yu, S.; Wang, C.; Yu, J.; Shi, W.; Deng, R.; Zhang, H. Precursor induced synthesis of hierarchical nanostructured ZnO. *Nanotechnology* **2006**, *17*, 3607–3612. [[CrossRef](#)] [[PubMed](#)]
96. Zhao, J.; Zou, X.; Zhou, L.; Feng, L.; Jin, P.; Liu, Y.; Li, G. Precursor-mediated synthesis and sensing properties of wurtzite ZnO microspheres composed of radially aligned porous nanorods. *Dalton Trans.* **2013**, *42*, 14357. [[CrossRef](#)] [[PubMed](#)]
97. Hong, Y.; Tian, C.; Jiang, B.; Wu, A.; Zhang, Q.; Tian, G.; Fu, H. Facile synthesis of sheet-like ZnO assembly composed of small ZnO particles for highly efficient photocatalysis. *J. Mater. Chem. A* **2013**, *1*, 5700. [[CrossRef](#)]
98. Jang, E.; Won, J.; Kim, Y.; Cheng, Z.; Choy, J. Synthesis of porous and nonporous ZnO nanobelt, multipod, and hierarchical nanostructure from Zn-HDS. *J. Solid State Chem.* **2010**, *183*, 1835–1840. [[CrossRef](#)]

99. Li, Y.; Che, Z.; Sun, X.; Dou, J.; Wei, M. Metal–organic framework derived hierarchical ZnO parallelepipeds as an efficient scattering layer in dye-sensitized solar cells. *Chem. Commun.* **2014**, *50*, 9769. [[CrossRef](#)] [[PubMed](#)]
100. Liao, D.L.; Badour, C.A.; Liao, B.Q. Preparation of nanosized TiO₂/ZnO composite catalyst and its photocatalytic activity for degradation of methyl orange. *J. Photochem. Photobiol. A Chem.* **2008**, *194*, 11–19. [[CrossRef](#)]
101. Lei, Y.; Zhao, G.; Liu, M.; Zhang, Z.; Tong, X.; Cao, T. Fabrication, Characterization, and Photoelectrocatalytic Application of ZnO Nanorods Grafted on Vertically Aligned TiO₂ Nanotubes. *J. Phys. Chem. C* **2009**, *113*, 19067–19076. [[CrossRef](#)]
102. Xiao, F. Construction of Highly Ordered ZnO–TiO₂ Nanotube Arrays (ZnO/TNTs) Heterostructure for Photocatalytic Application. *ACS Appl. Mater. Interfaces* **2012**, *4*, 7055–7063. [[CrossRef](#)] [[PubMed](#)]
103. Xiao, F.; Hung, S.; Tao, H.; Miao, J.; Yang, H.; Liu, B. Spatially branched hierarchical ZnO nanorod-TiO₂ nanotube array heterostructures for versatile photocatalytic and photoelectrocatalytic applications: Towards intimate integration of 1D-1D hybrid nanostructures. *Nanoscale* **2014**, *6*, 14950–14961. [[CrossRef](#)] [[PubMed](#)]
104. Pan, K.; Dong, Y.; Zhou, W.; Pan, Q.; Xie, Y.; Tian, G.; Wang, G. Facile Fabrication of Hierarchical TiO₂ Nanobelt/ZnO Nanorod Heterogeneous Nanostructure: An Efficient Photoanode for Water Splitting. *ACS Appl. Mater. Interfaces* **2013**, *5*, 8314–8320. [[CrossRef](#)] [[PubMed](#)]
105. Athauda, T.J.; Neff, J.G.; Sutherlin, L.; Butt, U.; Ozer, R.R. Systematic Study of the Structure–Property Relationships of Branched Hierarchical TiO₂/ZnO Nanostructures. *ACS Appl. Mater. Interfaces* **2012**, *4*, 6917–6926. [[CrossRef](#)] [[PubMed](#)]
106. Wang, W.W.; Zhu, Y.J.; Yang, L.X. ZnO–SnO₂ Hollow Spheres and Hierarchical Nanosheets: Hydrothermal Preparation, Formation Mechanism, and Photocatalytic Properties. *Adv. Funct. Mater.* **2007**, *17*, 59–64. [[CrossRef](#)]
107. Cheng, C.; Liu, B.; Yang, H.; Zhou, W.; Sun, L.; Chen, R.; Yu, S.; Zhang, J.; Gong, H.; Sun, H.; et al. Hierarchical Assembly of ZnO Nanostructures on SnO₂ Backbone Nanowires: Low-Temperature Hydrothermal Preparation and Optical Properties. *ACS Nano* **2009**, *3*, 3069–3076. [[CrossRef](#)] [[PubMed](#)]
108. Liu, S.; Yang, M.; Tang, Z.; Xu, Y. A nanotree-like CdS/ZnO nanocomposite with spatially branched hierarchical structure for photocatalytic fine-chemical synthesis. *Nanoscale* **2014**, *6*, 7193. [[CrossRef](#)] [[PubMed](#)]
109. Chang, Y.; Xu, J.; Zhang, Y.; Ma, S.; Xin, L.; Zhu, L.; Xu, C. Optical Properties and Photocatalytic Performances of Pd Modified ZnO Samples. *J. Phys. Chem. C* **2009**, *113*, 18761–18767. [[CrossRef](#)]
110. Georgekutty, R.; Seery, M.K.; Pillai, S.C. A Highly Efficient Ag-ZnO Photocatalyst: Synthesis, Properties, and Mechanism. *J. Phys. Chem. C* **2008**, *112*, 13563–13570. [[CrossRef](#)]
111. Ahmad, M.; Shi, Y.; Nisar, A.; Sun, H.; Shen, W.; Wei, M.; Zhu, J. Synthesis of hierarchical flower-like ZnO nanostructures and their functionalization by Au nanoparticles for improved photocatalytic and high performance Li-ion battery anodes. *J. Mater. Chem.* **2011**, *21*, 7723. [[CrossRef](#)]
112. Xia, W.; Mei, C.; Zeng, X.; Fan, G.; Lu, J.; Meng, X.; Shen, X. Nanoplate-Built ZnO Hollow Microspheres Decorated with Gold Nanoparticles and Their Enhanced Photocatalytic and Gas-Sensing Properties. *ACS Appl. Mater. Interfaces* **2015**, *7*, 11824–11832. [[CrossRef](#)] [[PubMed](#)]
113. Luo, Q.; Yu, X.; Lei, B.; Chen, H.; Kuang, D.; Su, C. Reduced Graphene Oxide-Hierarchical ZnO Hollow Sphere Composites with Enhanced Photocurrent and Photocatalytic Activity. *J. Phys. Chem. C* **2012**, *116*, 8111–8117. [[CrossRef](#)]
114. Zhang, W. Growth of ZnO nanowires on modified well-aligned carbon nanotube arrays. *Nanotechnology* **2006**, *17*, 1036–1040. [[CrossRef](#)] [[PubMed](#)]
115. Anandan, S.; Ohashi, N.; Miyauchi, M. ZnO-based visible-light photocatalyst: Band-gap engineering and multi-electron reduction by co-catalyst. *Appl. Catal. B Environ.* **2010**, *100*, 502–509. [[CrossRef](#)]
116. Hasnat, M.; Uddin, M.; Samed, A.; Alam, S.; Hossain, S. Adsorption and photocatalytic decolorization of a synthetic dye erythrosine on anatase TiO₂ and ZnO surfaces. *J. Hazard. Mater.* **2007**, *147*, 471–477. [[CrossRef](#)] [[PubMed](#)]
117. Peternel, I.T.; Koprivanac, N.; Božić, A.; Kušić, H. Comparative study of UV/TiO₂, UV/ZnO and photo-Fenton processes for the organic reactive dye degradation in aqueous solution. *J. Hazard. Mater.* **2007**, *148*, 477–484. [[CrossRef](#)] [[PubMed](#)]
118. Liu, Z.; Bai, H.; Xu, S.; Sun, D. Hierarchical CuO/ZnO “corn-like” architecture for photocatalytic hydrogen generation. *Int. J. Hydrog. Energy* **2011**, *36*, 13473–13480. [[CrossRef](#)]

119. Yang, X.; Wolcott, A.; Wang, G.; Sobo, A.; Fitzmorris, R.; Qian, F.; Zhang, J.; Li, Y. Nitrogen-Doped ZnO Nanowire Arrays for Photoelectrochemical Water Splitting. *Nano Lett.* **2009**, *9*, 2331–2336. [[CrossRef](#)] [[PubMed](#)]
120. Lv, R.; Wang, T.; Su, F.; Zhang, P.; Li, C.; Gong, J. Facile synthesis of ZnO nanopencil arrays for photoelectrochemical water splitting. *Nano Energy* **2014**, *7*, 143–150. [[CrossRef](#)]
121. Wolcott, A.; Smith, W.; Kuykendall, T.; Zhao, Y.; Zhang, J. Photoelectrochemical Study of Nanostructured ZnO Thin Films for Hydrogen Generation from Water Splitting. *Adv. Funct. Mater.* **2009**, *19*, 1849–1856. [[CrossRef](#)]
122. Zhang, C.; Shao, M.; Ning, F.; Xu, S.; Li, Z.; Wei, M.; Evans, D.G.; Duan, X. Au nanoparticles sensitized ZnO nanorod@nanoplatelet core–shell arrays for enhanced photoelectrochemical water splitting. *Nano Energy* **2015**, *12*, 231–239. [[CrossRef](#)]
123. Daneshvar, N.; Salari, D.; Khataee, A.R. Photocatalytic degradation of azo dye acid red 14 in water on ZnO as an alternative catalyst to TiO₂. *J. Photochem. Photobiol. A Chem.* **2004**, *162*, 317–322. [[CrossRef](#)]
124. Fujishima, A.; Zhang, X.; Tryk, D. TiO₂ photocatalysis and related surface phenomena. *Surface Sci. Rep.* **2008**, *63*, 515–582. [[CrossRef](#)]
125. Xiong, Z.; Zhang, L.L.; Ma, J.; Zhao, X.S. Photocatalytic degradation of dyes over graphene–gold nanocomposites under visible light irradiation. *Chem. Commun.* **2010**, *46*, 6099. [[CrossRef](#)] [[PubMed](#)]
126. Wu, T.; Liu, G.; Zhao, J. Photoassisted Degradation of Dye Pollutants. V. Self-Photosensitized Oxidative Transformation of Rhodamine B under Visible Light Irradiation in Aqueous TiO₂ Dispersions. *J. Phys. Chem. B* **1998**, *102*, 5845–5851. [[CrossRef](#)]
127. Zheng, Y.; Tao, X.; Hou, Q.; Wang, D.; Zhou, W.; Chen, J. Iodine-Doped ZnO Nanocrystalline Aggregates for Improved Dye-Sensitized Solar Cells. *Chem. Mater.* **2011**, *23*, 3–5. [[CrossRef](#)]
128. Wang, Y.; Fang, H.B.; Zheng, Y.Z.; Ye, R.; Tao, X.; Chen, J.F. Controllable assembly of well-defined monodisperse Au nanoparticles on hierarchical ZnO microspheres for enhanced visible-light-driven photocatalytic and antibacterial activity. *Nanoscale* **2015**, *7*, 19118–19128. [[CrossRef](#)] [[PubMed](#)]
129. DuChene, J.S.; Sweeny, B.C.; Johnston-Peck, A.C.; Su, D.; Stach, E.A.; Wei, W.D. Prolonged Hot Electron Dynamics in Plasmonic-Metal/Semiconductor Heterostructures with Implications for Solar Photocatalysis. *Angew. Chemie Int. Ed.* **2014**, *53*, 7887–7891. [[CrossRef](#)] [[PubMed](#)]
130. Yu, W.; Zhang, J.; Peng, T. New insight into the enhanced photocatalytic activity of N-, C- and S-doped ZnO photocatalysts. *Appl. Catal. B Environ.* **2016**, *181*, 220–227. [[CrossRef](#)]
131. Xu, F.; Volkov, V.; Zhu, Y.; Bai, H.; Rea, A.; Valappil, N.; Su, W.; Gao, X.; Kuskovsky, I.; Matsui, H. Long Electron–Hole Separation of ZnO–CdS Core–Shell Quantum Dots. *J. Phys. Chem. C* **2009**, *113*, 19419–19423. [[CrossRef](#)]
132. Eley, C.; Li, T.; Liao, F.; Fairclough, S.; Smith, J.; Smith, G.; Tsang, S. Nanojunction-Mediated Photocatalytic Enhancement in Heterostructured CdS/ZnO, CdSe/ZnO, and CdTe/ZnO Nanocrystals. *Angew. Chemie Int. Ed.* **2014**, *53*, 7838–7842. [[CrossRef](#)] [[PubMed](#)]
133. Zhang, A.; Wang, W.; Pei, D.; Yu, H. Degradation of refractory pollutants under solar light irradiation by a robust and self-protected ZnO/CdS/TiO₂ hybrid photocatalyst. *Water Res.* **2016**, *92*, 78–86. [[CrossRef](#)] [[PubMed](#)]
134. Linic, S. Christopher and D.B. Ingram, Plasmonic-metal nanostructures for efficient conversion of solar to chemical energy. *Nat. Mater.* **2011**, *10*, 911–921. [[CrossRef](#)] [[PubMed](#)]
135. Tian, Y.; Tatsuma, T. Mechanisms and Applications of Plasmon-Induced Charge Separation at TiO₂ Films Loaded with Gold Nanoparticles. *J. Am. Chem. Soc.* **2005**, *127*, 7632–7637. [[CrossRef](#)] [[PubMed](#)]
136. Jiang, J.; Li, H.; Zhang, L. New Insight into Daylight Photocatalysis of AgBr@Ag: Synergistic Effect between Semiconductor Photocatalysis and Plasmonic Photocatalysis. *Chem. Eur. J.* **2012**, *18*, 6360–6369. [[CrossRef](#)] [[PubMed](#)]
137. Awazu, K.; Fujimaki, M.; Rockstuhl, C.; Tominaga, J.; Murakami, H.; Ohki, Y.; Yoshida, N.; Watanabe, T. A Plasmonic Photocatalyst Consisting of Silver Nanoparticles Embedded in Titanium Dioxide. *J. Am. Chem. Soc.* **2008**, *130*, 1676–1680. [[CrossRef](#)] [[PubMed](#)]
138. Kumar, M.K.; Krishnamoorthy, S.; Tan, L.K.; Chiam, S.Y.; Tripathy, S.; Gao, H. Field Effects in Plasmonic Photocatalyst by Precise SiO₂ Thickness Control Using Atomic Layer Deposition. *ACS Catal.* **2011**, *1*, 300–308. [[CrossRef](#)]

139. Wang, P.; Huang, B.; Dai, Y.; Whangbo, M.H. Plasmonic photocatalysts: harvesting visible light with noble metal nanoparticles. *Phys. Chem. Chem. Phys.* **2012**, *14*, 9813–9825. [[CrossRef](#)] [[PubMed](#)]
140. Chen, K.; Pu, Y.; Chang, K.; Liang, Y.; Liu, C.; Yeh, J.; Shih, H.; Hsu, Y. Ag-Nanoparticle-Decorated SiO₂ Nanospheres Exhibiting Remarkable Plasmon-Mediated Photocatalytic Properties. *J. Phys. Chem. C* **2012**, *116*, 19039–19045. [[CrossRef](#)]
141. Zhang, N.; Liu, S.; Xu, Y. Recent progress on metal core@semiconductor shell nanocomposites as a promising type of photocatalyst. *Nanoscale* **2012**, *4*, 2227–2238. [[CrossRef](#)] [[PubMed](#)]
142. Ren, S.; Wang, B.; Zhang, H.; Ding, P.; Wang, Q. Sandwiched ZnO@Au@Cu₂O Nanorod Films as Efficient Visible-Light-Driven Plasmonic Photocatalysts. *ACS Appl. Mater. Interfaces* **2015**, *7*, 4066–4074. [[CrossRef](#)] [[PubMed](#)]
143. Barpuzary, D.; Khan, Z.; Vinothkumar, Z.; De, M.; Qusheshi, M. Hierarchically Grown Urchinlike CdS@ZnO and CdS@Al₂O₃ Heteroarrays for Efficient Visible-Light-Driven Photocatalytic Hydrogen Generation. *J. Phys. Chem. C* **2012**, *116*, 150–156. [[CrossRef](#)]
144. Kargar, A.; Sun, K.; Jing, Y.; Choi, C.; Jeong, H.; Jung, G.Y.; Jin, S.; Wang, D. 3D Branched Nanowire Photoelectrochemical Electrodes for Efficient Solar Water Splitting. *ACS Nano* **2013**, *7*, 9407–9415. [[CrossRef](#)] [[PubMed](#)]
145. Kargar, A.; Jing, Y.; Kim, S.J.; Riley, C.T.; Pan, X.; Wang, D. ZnO/CuO Heterojunction Branched Nanowires for Photoelectrochemical Hydrogen Generation. *ACS Nano* **2013**, *7*, 11112–11120. [[CrossRef](#)] [[PubMed](#)]
146. Hsu, M.; Chang, C.; Weng, H. Efficient H₂ Production Using Ag₂S-Coupled ZnO@ZnS Core–Shell Nanorods Decorated Metal Wire Mesh as an Immobilized Hierarchical Photocatalyst. *ACS Sustain. Chem. Eng.* **2016**, *4*, 1381–1391. [[CrossRef](#)]
147. Yu, Z.B.; Xie, Y.P.; Liu, G.; Lu, G.Q.; Ma, X.L.; Cheng, H.M. Self-assembled CdS/Au/ZnO heterostructure induced by surface polar charges for efficient photocatalytic hydrogen evolution. *J. Mater. Chem. A* **2013**, *1*, 2773. [[CrossRef](#)]
148. Maeda, K.; Xiong, A.; Yoshinaga, T.; Iketa, T.; Sakamoto, N.; Hisatomi, T.; Takashima, M.; Lu, D.; Kanehara, M.; Setoyama, T.; et al. Photocatalytic Overall Water Splitting Promoted by Two Different Cocatalysts for Hydrogen and Oxygen Evolution under Visible Light. *Angew. Chemie Int. Ed.* **2010**, *49*, 4096–4099. [[CrossRef](#)] [[PubMed](#)]
149. Thiyagarajan, P.; Ahn, H.J.; Lee, J.S.; Yoon, J.C.; Jang, J.H. Hierarchical Metal/Semiconductor Nanostructure for Efficient Water Splitting. *Small* **2013**, *13*, 2341–2347. [[CrossRef](#)] [[PubMed](#)]
150. Zhang, X.; Liu, Y.; Kang, Z. 3D Branched ZnO Nanowire Arrays Decorated with Plasmonic Au Nanoparticles for High-Performance Photoelectrochemical Water Splitting. *ACS Appl. Mater. Interfaces* **2014**, *6*, 4480–4489. [[CrossRef](#)] [[PubMed](#)]



© 2016 by the authors; licensee MDPI, Basel, Switzerland. This article is an open access article distributed under the terms and conditions of the Creative Commons Attribution (CC-BY) license (<http://creativecommons.org/licenses/by/4.0/>).